

RESEARCH

Open Access



Role of TDP2 in the repair of DNA damage induced by the radiomimetic drug Bleomycin

Naoto Shimizu^{1,4}, Kazuki Izawa², Mubasshir Washif³, Ryosuke Morozumi^{1,2}, Kouji Hirota³ and Masataka Tsuda^{1,2*}

Abstract

Background Bleomycin (Bleo) is a glycopeptide with potent antitumor activity that induces DNA double-strand breaks (DSBs) through free radical generation, similar to ionizing radiation (IR). Therefore, Bleo is considered a radiomimetic drug. However, differences in DNA repair mechanisms between IR- and Bleo-induced DNA damage have not been fully elucidated. Therefore, in the present study, we examined a panel of repair-deficient human TK6 cell lines to elucidate the relative contributions of individual repair factors.

Results Our comprehensive profiling indicated that both non-homologous end joining (NHEJ) and homologous recombination (HR) contributed to DSB repair induced by X-rays and Bleo. Furthermore, tyrosyl-DNA phosphodiesterase (TDP)-related repair was a significant factor for cellular sensitivity to Bleo treatment. *TDP1*^{-/-}/*TDP2*^{-/-} cells exhibited greater sensitivity to Bleo than *TDP1*^{-/-} or *TDP2*^{-/-} cells, but not to X-rays. In addition, we determined whether TDP2 is involved in the repair of Bleo-induced DSBs using a neutral comet assay. In *TDP1*-deficient cells, knockout of *TDP2* resulted in a significant delay in the repair kinetics of DSBs induced by Bleo, but not by X-rays.

Conclusions The contribution of the TDP-related pathway to DSB repair significantly differed between IR and radiomimetic drugs. The discovery of this novel TDP2-dependent repair of DSBs resulting from radiomimetic drug exposure indicates that TDP1 and TDP2 inhibition in combination with radiomimetic drugs represents a strategy for cancer treatment.

Keywords Radiomimetic drugs, Bleomycin, Ionizing radiation, DNA double-strand breaks, TK6, Tyrosyl-DNA phosphodiesterase

Background

Bleomycin (Bleo) is a glycopeptide that exhibits potent antitumor activity against lymphomas; malignant germ cell tumors; and carcinomas of the skin, head, and neck [1, 2]. Bleo generates free radicals in DNA, which results in DNA double-strand breaks (DSBs) with a biological effect similar to those induced by ionizing radiation (IR) [3]. Bleo induces DSBs and single-strand breaks (SSBs) in a ratio of approximately 1:6–1:20 [4, 5], whereas IR exposure causes DSBs and SSBs in a ratio of approximately 1:20. Bleo is a radiomimetic drug; however, sensitivity to Bleo is not necessarily correlated with radiation

*Correspondence:

Masataka Tsuda
tsudam@nihs.go.jp

¹Program of Biomedical Science, Graduate School of Integrated Sciences for Life, Hiroshima University, Higashi-Hiroshima, Japan

²Division of Genome Safety Science, National Institute of Health Sciences, Kawasaki, Kanagawa, Japan

³Department of Chemistry, Graduate School of Science, Tokyo Metropolitan University, Minamiosawa 1-1, Hachioji-shi, Tokyo 192-0397, Japan

⁴Present address: Division of Cell-Based Therapeutic Products, National Institute of Health Sciences, Kawasaki, Kanagawa, Japan



© The Author(s) 2025. **Open Access** This article is licensed under a Creative Commons Attribution 4.0 International License, which permits use, sharing, adaptation, distribution and reproduction in any medium or format, as long as you give appropriate credit to the original author(s) and the source, provide a link to the Creative Commons licence, and indicate if changes were made. The images or other third party material in this article are included in the article's Creative Commons licence, unless indicated otherwise in a credit line to the material. If material is not included in the article's Creative Commons licence and your intended use is not permitted by statutory regulation or exceeds the permitted use, you will need to obtain permission directly from the copyright holder. To view a copy of this licence, visit <http://creativecommons.org/licenses/by/4.0/>. The Creative Commons Public Domain Dedication waiver (<http://creativecommons.org/publicdomain/zero/1.0/>) applies to the data made available in this article, unless otherwise stated in a credit line to the data.

sensitivity in head and neck squamous cell lines [6]. One possible explanation for this phenomenon is that different DNA repair pathways may operate in response to DNA damage induced by IR and Bleo.

It is well established that both IR and Bleo induce DNA damage, and the differences in the lesions they produce have been extensively characterized. IR deposits energy into molecules, leading to the cleavage of chemical bonds; as it traverses cells, it disrupts covalent bonds within genomic DNA. Consequently, IR induces a range of DNA lesions, including base modifications, SSBs, DSBs, and DNA-protein crosslinks (DPCs) [7]. In contrast, Bleo becomes activated upon binding to Fe(II), followed by the binding of oxygen and reduction by a reductant. This activated Bleo induces DSBs with characteristic 3'-phosphoglycolate (3'-PG) and 5'-phosphate ends and also generates 4'-oxidized abasic sites, where the base is lost and the sugar backbone is altered [5]. These lesions may disrupt essential cellular processes such as replication and transcription. Thus, although IR and Bleo induce distinct spectra of DNA damage, it remains unclear how these differences affect the mechanisms that repair DNA damage induced by each agent.

The DSB repair mechanism has primarily been elucidated using IR [7]. Eukaryotic cells employ two major DSB repair pathways that play a significant role in preventing cell death: homologous recombination (HR) and nonhomologous end joining (NHEJ) [8, 9]. HR involves several steps, including end resection on the DSB strand, homology search, strand invasion into the homologous template, and DNA repair synthesis [10]. RAD54 is an important protein that promotes strand invasion during HR [11]. In NHEJ, the broken ends of two DSBs are directly rejoined without the use of homologous templates. The Ku heterodimer initiates the process, which results in the activation of the DNA-dependent protein kinase catalytic subunit (DNA-PKcs) and recruitment of DNA ligase 4 (LIG4) to seal the broken ends [12]. During the G1 phase, 53BP1 promotes NHEJ [13]. The base damage is converted into an SSB (DNA nick) as an intermediate step in the repair process [14]. With a DNA nick, poly (ADP-ribose) polymerase 1 (PARP-1) gets activated and poly (ADP-ribosyl) ates several proteins, including itself [15, 16]. PARP-1 predominantly interacts with the X-ray repair cross-complementing group 1 (XRCC1) protein [17, 18]. At the DNA damage site, XRCC1 contributes to repair by recruiting DNA polymerase (POL) β , which is involved in gap-filling synthesis and removal of the 5'-blocking group [19, 20]. The repair of DPCs induced by formaldehyde and etoposide is mediated by the metalloprotease SPRTN [21]. The repair of DPCs induced by topoisomerase inhibitors and formaldehyde is initiated not only by SPRTN but also by the proteasome [19]. Notably, *SPRTN*^{-/-} cells are not sensitive to IR,

suggesting that SPRTN does not participate in the repair of IR-induced DPCs [22]; however, the overall differences in the contributions of these factors to the repair of DNA damage induced by IR and Bleo remains unclear.

A set of isogenic human TK6 cells that are DNA repair mutant clones and possess functional p53 comparable to normal human tissues exhibiting rapid proliferation (13 h/cell cycle) has been established [23]. Using this mutant panel, the role of individual repair pathways following IR irradiation in cell survival was examined between normoxic and hypoxic cells [22]. Recently, we used comprehensive profiling to demonstrate that the tyrosyl-DNA phosphodiesterase (TDP)-related repair pathway is a primary contributor to the repair of DNA damage induced by Camptothecin (CPT) [24].

In the present study, we compared the sensitivity of a panel of DNA repair-deficient TK6 cell lines to X-rays and Bleo. Distinct sensitivity patterns were observed among TDP-related repair mutant cells. Interestingly, *TDPI*^{-/-}/*TDP2*^{-/-} cells exhibited increased sensitivity to Bleo, but not to X-rays, compared with single mutant cells. The absence of TDP2 enhanced the delay in DSB repair in *TDPI*^{-/-} cells following treatment. These findings suggest a novel role of TDP2 in DSB repair induced by Bleo.

Materials and methods

Cell culture

Human lymphoblast TK6 cells [25] were supplied by Dr. Shunichi Takeda and Dr. Hiroyuki Sasanuma (Department of Radiation Genetics, Graduate School of Medicine, Kyoto University; Table 1). The cells were cultured in RPMI-1640 medium (189-02025, Wako, Osaka, Japan) supplemented with 5% heat-inactivated horse serum, L-glutamine (16948-04, Nacalai Tesque, Kyoto, Japan), 0.2 mg/mL sodium pyruvate (P2256, Sigma-Aldrich, Steinheim, Germany), 100 U/mL penicillin, and 100 μ g/mL streptomycin (168-23191, Nacalai Tesque, Kyoto, Japan) and maintained at 37 °C in a humidified atmosphere containing 5% CO₂ as previously described [22, 26].

Cell survival

X-rays were generated by an OHMic OM-303 M X-ray generator (70 kV, 3 mA, 0.2 mm Al filter). Bleomycin sulfate (Bleo; B3972) was purchased from TOKYO CHEMICAL INDUSTRY (Tokyo, Japan). Cells were either irradiated with X-rays or treated with Bleo for 3 h at 37 °C. The cells were seeded in triplicate in six-well plates with 5 mL/well of 1.5% (w/v) methylcellulose (M0387, Sigma-Aldrich, Steinheim, Germany) and D-MEM/Ham's F-12 (042-30555, Wako, Osaka, Japan) supplemented with 10% horse serum. The number of colonies was counted at day 10 to 14 [26-28].

Table 1 Panel of cell lines used in this study

Genotype	Functions of the deleted gene(s)	References
<i>TDP1</i> ^{-/-}	TDP-related repair	[36]
<i>TDP2</i> ^{-/-}	TDP-related repair	[34, 36]
<i>TDP2</i> ^{E152Q/E152Q}	TDP-related repair	[24]
<i>TDP1</i> ^{-/-} / <i>TDP2</i> ^{-/-}	TDP-related repair	[30, 37]
<i>TDP1</i> ^{-/-} / <i>TDP2</i> ^{E152Q/E152Q}	TDP-related repair	[24]
<i>53BP1</i> ^{-/-}	DSB repair (NHEJ)	[38]
<i>DNA-PKCS</i> ^{-/-}	DSB repair (NHEJ)	[39]
<i>LIG4</i> ^{-/-}	DSB repair (NHEJ)	[39]
<i>RAD54</i> ^{-/-}	DSB repair (HR)	[39]
<i>RAD54</i> ^{-/-} / <i>LIG4</i> ^{-/-}	DSB repair (HR/NHEJ)	[39]
<i>XRCC1</i> ^{-/-}	BER	[40]
<i>PARP1</i> ^{-/-}	BER	[37]
<i>XPA</i> ^{-/-}	NER	[26]
<i>SPRTN</i> ^{-/-}	DPC repair, TLS	[41]
<i>RAD18</i> ^{-/-}	TLS	[28]
<i>POLη</i> ^{-/-}	TLS	[26]
<i>MLH1</i> ^{-/-}	MMR	[42]
<i>MLH3</i> ^{-/-}	MMR	[42]
<i>POLε</i> ^{exo-/-}	Proofreading of replicative polymerase	[28]

BER base excision repair; DPC DNA-protein crosslink; HR homologous recombination; MMR mismatch repair; NER nucleotide excision repair; NHEJ nonhomologous end joining; TDP tyrosyl-DNA phosphodiesterase; TLS translesion DNA synthesis

Neutral comet assays

Cells were either irradiated with 20 Gy X-rays or treated with 400 µg/mL Bleo for 30 min at 37 °C, and incubated in drug-free media for 180 min. The cells were embedded in agarose, treated with lysis buffer, and electrophoresed as previously described [24]. The slides were observed under a fluorescence microscope (TE2000; Nikon, Tokyo, Japan) at 200× magnification. OpenComet software was used to measure the tail moments from 50 cells/sample [29].

Statistical analysis

Significant differences were identified using Tukey's multiple comparison test, ANOVA, and Student's t-test implemented in *scipy* (1.6.2).

Biochemical analysis of 3'-PG processing

The 3'-PG oligonucleotide (5'-TCCCCAACTAACATG AACTCGACG) was purchased from Eurogentec (Seraing, Belgium). The 3'-PG oligonucleotide was 5'-labeled with ³²P using [γ-³²P] ATP and T4 polynucleotide kinase (2021 S, TAKARA). The labeled DNA substrates were incubated with the indicated concentrations of recombinant human TDP1 (ab131921, Abcam, Cambridge, UK) or TDP2 (#TG2003H, TopoGEN, Co, USA) for 30 min at 37 °C in 5 µl of reaction buffer. Reactions were terminated by adding one volume of gel loading buffer (formamide containing 2.5 mM EDTA). Samples were separated

using 20% denaturing polyacrylamide gel containing 7 M urea in TBE buffer (89 mM Tris, 89 mM boric acid, and 2 mM EDTA). Following electrophoresis, the radioactivity of the gel was measured using a Typhoon FLA9500 (GE Healthcare Life Sciences).

Results

Contribution of TDP-dependent repair to Bleo-induced DNA damage response

The sensitivity of a panel of DNA repair-deficient TK6 cell lines, consisting of 19 mutant cell lines, was examined using X-rays and Bleo (Table 1). The doses resulting in 10% survival (LD10) were calculated. Figure 1 shows the ratio of LD10 values between individual isogenic mutants and *wild-type* cells on a logarithmic scale. Our findings revealed that NHEJ-deficient (*LIG4*^{-/-}, *DNA-PKCS*^{-/-}, and *53BP1*^{-/-}) cells were sensitive to both X-rays [22] and Bleo. In contrast, HR deficiency resulted in hypersensitivity to X-rays but minimal sensitivity to Bleo. These findings suggest that while both NHEJ and HR contribute equally to X-ray-induced DSB repair, NHEJ plays a more prominent role in repairing DSBs induced by Bleo compared with HR. Furthermore, *RAD54*^{-/-}/*LIG4*^{-/-} cells exhibited greater sensitivity to X-rays and Bleo than *RAD54*^{-/-} or *LIG4*^{-/-} cells. Thus, DSBs are the major type of DNA damage induced by both X-rays and Bleo. Overall, the sensitivity profiles of these agents were similar (Fig. 1). Interestingly, TDP-related mutant cells displayed distinct sensitivity profiles between X-rays and Bleo. While *TDP1*^{-/-} cells were sensitive to Bleo, they exhibited little sensitivity to X-rays. In addition, *TDP1*^{-/-}/*TDP2*^{-/-} cells were more sensitive to Bleo than single mutant cells. The Bleo sensitivity of TDP-related repair mutant cells is similar to CPT sensitivity of the cells [24, 30]. CPT is a well-known anticancer agent that inhibits DNA topoisomerase 1 (TOP1), resulting in the trapping of TOP1-DNA cleavage complexes (TOP1ccs) [31, 32] that are repaired by TDP1 [33]. TDP2 primarily repairs trapped TOP2-DNA cleavage complexes (TOP2ccs) [34], and TDP2 repairs TOP1ccs in the absence of TDP1 [30, 35]. Therefore, TDP2 appears to be involved in the repair of Bleo and CPT-induced DNA damage in the absence of TDP1.

We previously identified the critical Glu152 residue in TDP2, which is responsible for binding and stabilizing the catalytically essential Mg²⁺ required for repairing both trapped TOP1ccs and TOP2ccs [24]. In TDP1-deficient human TK6 cells, but not *wild-type* cells, a Glu152Gln alteration in both alleles of *TDP2* resulted in a significant increase in Bleo sensitivity, whereas X-ray sensitivity was unaffected (Fig. 1). These data indicated the important role of Mg²⁺ binding to TDP2 in the repair of not only trapped topoisomerases but also Bleo-induced DNA damage.

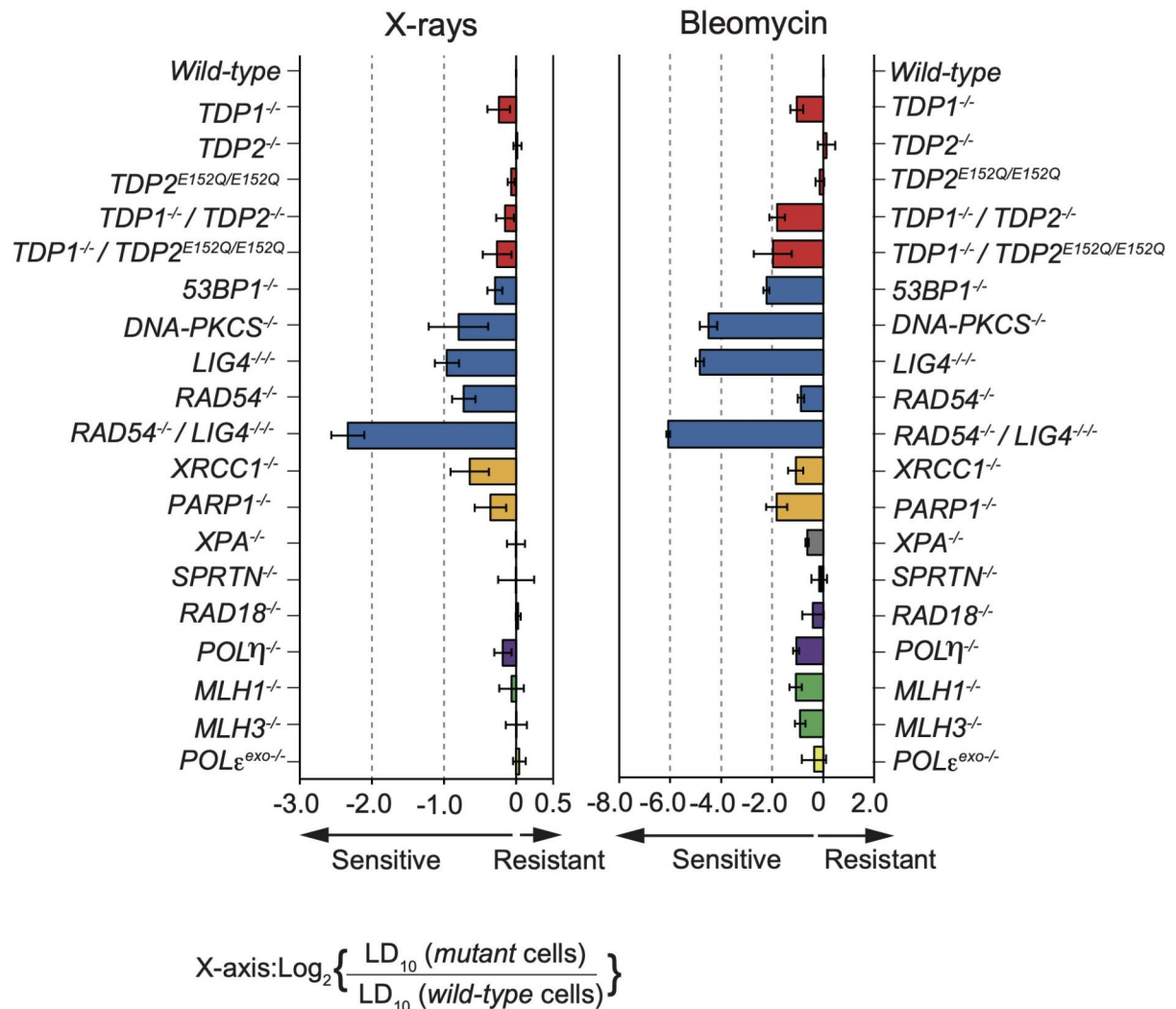


Fig. 1 X-rays and Bleo sensitivity profiles of selected DNA repair-deficient TK6 cells. The sensitivity of the mutant cells relative to *wild-type* cells was determined as described in the Materials and Methods. Negative and positive scores indicate the sensitivity and resistance of the given cell lines, respectively. Relative sensitivity was computed as follows: $\text{Log}_2 \left[\frac{\text{LD}_{10} (\text{mutant cells})}{\text{LD}_{10} (\text{wild-type cells})} \right]$. Each bar is colored based on the DNA repair function category: red, TDP-related repair; blue, DSB repair; orange, base excision repair (BER); gray, nucleotide excision repair (NER); black, DPC repair; purple, translesion synthesis (TLS); green, mismatch repair (MMR); and yellow, proofreading of replicative polymerase. Error bars indicate standard deviations of the mean of three independent assays

Assessment of DSB repair kinetics in TDP-related mutant cells following X-ray exposure

We hypothesized that TDP2 is specifically involved in a novel repair pathway for DSBs induced by Bleo, not by X-rays, in the absence of TDP1. The kinetics of DSB repair can be monitored using a neutral comet assay [43]. To investigate DSB repair kinetics, we irradiated *wild-type*, *TDP1*^{-/-}, *TDP2*^{-/-}, *TDP2*^{E152Q/E152Q}, *TDP1*^{-/-}/*TDP2*^{-/-}, and *TDP1*^{-/-}/*TDP2*^{E152Q/E152Q} cells. These cells were then allowed to recover in a drug-free medium for

180 min. Figure 2A shows typical images from a neutral comet assay. We analyzed 50 cell images per sample and plotted individual comet tail moments (an arbitrary measure of DSB). In all cell types, X-ray exposure caused an increase in the tail moment (Fig. 2B). Due to the observed variation in tail moments among mutants following X-ray exposure (Supplementary Table 1, Fig. S1A), we applied data standardization for the analysis of DSB repair capacity (Fig. 2C). At 180 min after X-ray exposure, the remaining DSBs were similar among *wild-type*, *TDP1*^{-/-},

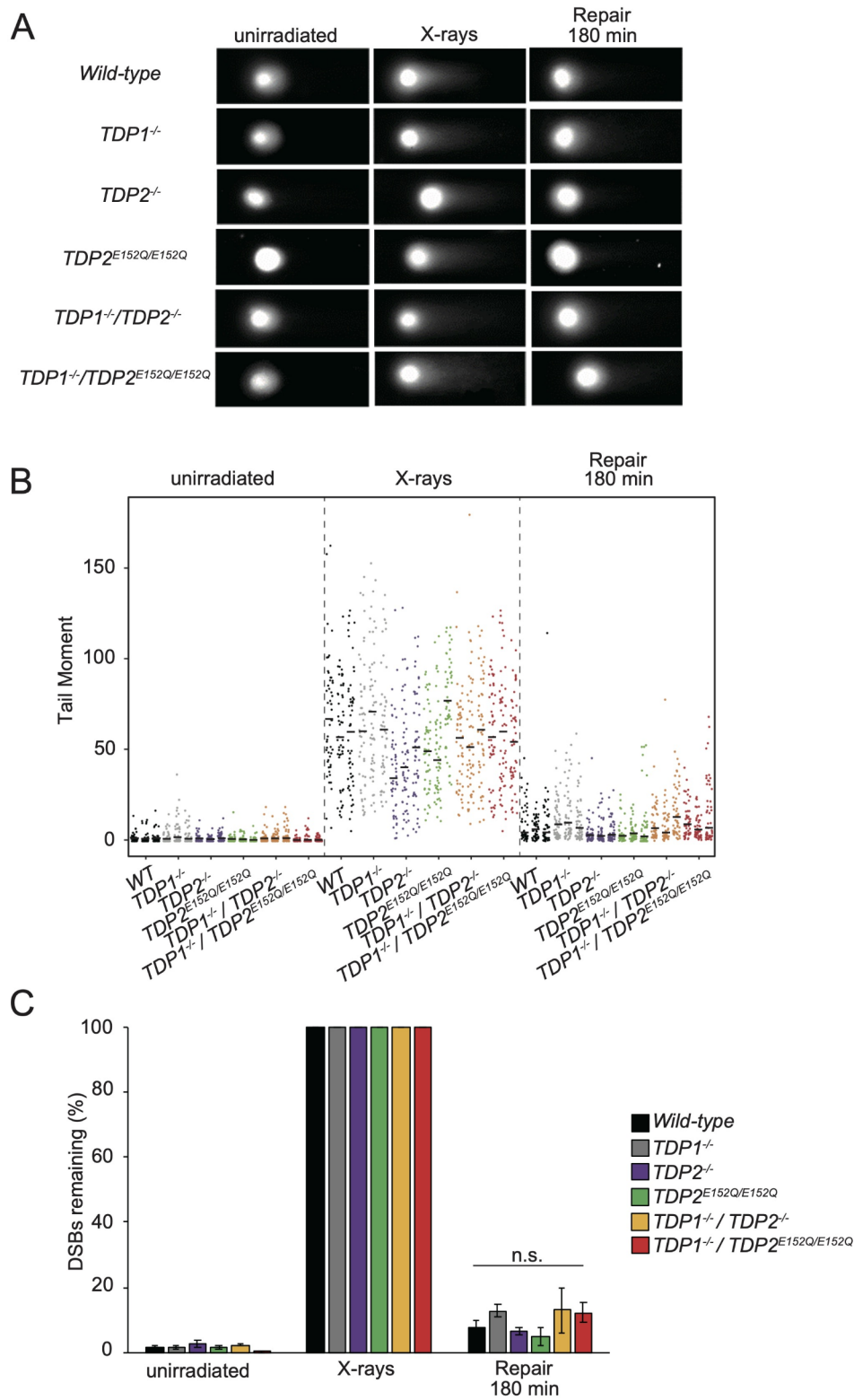


Fig. 2 (See legend on next page.)

(See figure on previous page.)

Fig. 2 Repair kinetics of DSBs in X-ray-irradiated cells. **A** Typical neutral comet images. The indicated cells were irradiated with and without X-rays, incubated in medium for 180 min, and analyzed for DSBs using neutral comet assays. The images below the X-rays show the samples prepared immediately after X-ray irradiation (0 min repair). **B** Tail moments (raw data) of irradiated cells in neutral comet assays. In total, we assessed 50 cells/sample and conducted experiments in triplicate for each cell type. Tail moments of different cells of each cell type from three experiments are plotted vertically in three separate columns. Lines indicate median tail moments. **C** Median tail moments were quantified for 50 cells/sample/experiment and standardized to those after 0 min of repair, bars on X-rays. DSBs remaining are presented as a percentage of the remaining damage. Error bars are standard deviations of the mean of three independent assays. Significant differences were identified using an ANOVA: n.s. = not significant. Median tail moments before standardization are shown in Fig. S1A

TDP1^{-/-}/*TDP2*^{-/-}, and *TDP1*^{-/-}/*TDP2*^{E152Q/E152Q} cells ($p > 0.005$, ANOVA), indicating that *TDP2* knockout in *TDP1*^{-/-} cells did not significantly affect DSB repair kinetics. These results indicate that *TDP1* and *TDP2* do not significantly contribute to the repair of DSB caused by X-ray exposure.

Delayed DSB repair kinetics of *TDP1*^{-/-}/*TDP2*^{-/-} cells following Bleo treatment

Next, we examined the repair kinetics of Bleo-induced DSBs in *wild-type*, *TDP1*^{-/-}, *TDP2*^{-/-}, *TDP2*^{E152Q/E152Q}, *TDP1*^{-/-}/*TDP2*^{-/-}, and *TDP1*^{-/-}/*TDP2*^{E152Q/E152Q} cells. These cells were treated with 400 µg/mL Bleo for 30 min and allowed to recover in a drug-free medium for 180 min. Figure 3A shows typical images from a neutral comet assay. In all cell types, Bleo treatment caused an increase in the tail moment (Fig. 3B). Due to the observed variation in tail moments among mutants following Bleo treatment (Supplementary Table 2, Fig. S1B), we applied data standardization for the analysis of DSB repair capacity (Fig. 3C). At 180 min after Bleo treatment, significant differences in the remaining DSBs were observed among *wild-type*, *TDP1*^{-/-}, *TDP1*^{-/-}/*TDP2*^{-/-}, and *TDP1*^{-/-}/*TDP2*^{E152Q/E152Q} cells ($p < 0.005$, ANOVA). Compared with *TDP1*^{-/-} cells, *TDP1*^{-/-}/*TDP2*^{-/-} cells exhibited a significant delay in DSB repair (t-test, Fig. 3C). Thus, *TDP1* and *TDP2* perform overlapping functions in the repair of Bleo-induced DSBs.

In addition, *TDP1*^{-/-}/*TDP2*^{E152Q/E152Q} cells exhibited a significant delay in DSB repair compared with *TDP1*^{-/-} cells (t-test, Fig. 3C). Therefore, Glu152 of *TDP2* plays a pivotal role in the repair of Bleo-induced DSBs in the absence of *TDP1*.

Bleo predominantly induces blunt-ended and 5'-staggered 3'-PG DSBs. Previous studies have demonstrated *TDP1*'s role in removing 3'-PG from DNA in biochemical experiments [44–47]. However, whether *TDP2* can also remove 3'-PG remains unclear. Thus, we conducted biochemical experiments using recombinant human *TDP2* and a single-stranded DNA substrate harboring a 3'-PG end (Fig. S2A). We first optimized buffer conditions for *TDP1* activity, identifying Buffer A—50 mM Tris-HCl (pH 7.5), 1 mM DTT, 25 mM KCl, and 0.1 mg/ml BSA—as most effective for 3'-PG removal (Fig. S2B). We then tested *TDP2* under the same conditions as *TDP1*; however, we did not detect any 3'-PG removal (Fig. S2C).

Based on these biochemical findings, we were unable to conclusively determine whether *TDP2* is involved in 3'-PG removal.

Discussion

In this study, we confirmed that both NHEJ and HR facilitated DSB repair induced by X-rays and Bleo. Furthermore, we identified *TDP2* as a susceptible gene following treatment with radiomimetic drugs, but not with X-rays, in the absence of *TDP1*.

This study provides significant insights into the DNA repair pathways in response to Bleo-induced DNA damage. Our results demonstrate that NHEJ is the predominant pathway contributing to the repair of Bleo-induced DSBs. This conclusion is supported by the pronounced sensitivity of NHEJ-deficient cells (*LIG4*^{-/-}, *DNA-PKcs*^{-/-}, and *53BP1*^{-/-}) to Bleo treatment, as shown in Fig. 1, underscoring the critical role of NHEJ in DNA repair following exposure to Bleo. Moreover, the greater sensitivity of *RAD54*^{-/-}/*LIG4*^{-/-} cells compared with each single mutant cell indicates that HR also plays a significant role in repairing Bleo-induced DNA damage (Fig. 1). This additive effect suggests that HR functions alongside NHEJ to facilitate DSB repair, highlighting the collaborative contributions of these pathways to cell survival after Bleo treatment.

In addition to the roles of NHEJ and HR, our findings reveal a crucial contribution of *TDP1* to the repair of Bleo-induced DSBs. *TDP1*^{-/-} cells, but not *TDP2*^{-/-} cells, exhibited increased sensitivity to Bleo and a delay in DSB repair, indicating that *TDP1* is involved in the repair of DSBs generated by Bleo treatment in *wild-type* cells. Furthermore, the *TDP1*^{-/-}/*TDP2*^{-/-} cells showed even greater sensitivity to Bleo and a more pronounced delay in DSB repair compared with *TDP1*^{-/-} cells alone. This suggests that in the absence of *TDP1*, *TDP2*, along with NHEJ and HR, contributes to the repair of Bleo-induced damage. *TDP2* may act as a backup mechanism for processing DNA termini when *TDP1* is absent. Overall, these findings indicate that Bleo-induced DSB ends contain lesions recognized by *TDP1* and *TDP2*. Once these lesions are removed by *TDP1* or *TDP2*, the resulting DSBs may subsequently be repaired by HR or NHEJ.

We found that *TDP1*^{-/-}/*TDP2*^{-/-} cells exhibited greater sensitivity to Bleo than *TDP1*^{-/-} or *TDP2*^{-/-} single mutants, but not to X-rays. This discrepancy may be

explained by the distinct DNA damage profiles induced by Bleo versus IR. Unlike IR, Bleo predominantly generates 3'-PG ends at DNA breaks, requiring specific repair mechanisms [5]. In addition, TDP1 processes 3'-PG [44–46, 48, 49] and suppresses the misjoining of radiomimetic DSBs [50]. Consequently, we sought to determine whether TDP2 is directly involved in removing 3'-PG. However, it is not known that any method exists for specifically labeling Bleo-induced 3'-PG, making direct analysis of 3'-PG removal at the cellular level unfeasible. Therefore, we carried out biochemical experiments using recombinant human TDP2 and a DNA substrate harboring a 3'-PG end (Fig. S2A). Under these conditions, TDP1 processed 3'-PG in vitro (Fig. S2B); however, TDP2 failed to do so (Fig. S2C). These results suggest several possibilities. First, TDP2 may simply lack 3'-PG removal activity in vitro, instead participating in the repair of other minor lesions, such as DPCs. Bleo is activated upon binding to oxygen molecules, potentially leading to DNA–protein crosslinking. This minor form of damage could be a target for TDP2. Second, the optimal buffer conditions for TDP1 and TDP2 may differ. This can be explained by the fact that TDP2's 3'-TDP activity requires a divalent metal ion, whereas TDP1's does not [24]. Therefore, we hypothesized that TDP2's 3'-PG processing activity also depends on a divalent metal ion. However, TDP2 did not exhibit 3'-PG processing activity in buffers containing Mg^{2+} (buffer B, C, D, F, G, H) (Fig. S2C), suggesting that the Mg^{2+} concentration or the pH may not have been optimized for this reaction. Third, TDP2 may require additional cofactors to act on 3'-PG; for example, a chaperon may help TDP2 access to the 3'-PG site or promote the catalytic activity of TDP2 for 3'-PG in *TDP1*^{-/-} cells. In the second and third scenarios, TDP2 could potentially remove 3'-PG damage in the absence of TDP1 in cells, functioning as a backup mechanism for this particular lesion. By contrast, IR-induced breaks comprise diverse and complex lesions that are repaired by a broader set of enzymes involved in HR or NHEJ, making TDP2's specialized function less critical for IR-induced damages. Nonetheless, these possibilities remain speculative, and further studies are needed to clarify the precise role of TDP2 in repairing 3'-PG damage.

We previously suggested that the inhibition of TDP2 combined with a TOP1 inhibitor and chain-terminating nucleoside analogs may be an effective strategy for tumor treatment [30]. We also suggested that enhancing Mg^{2+} chelating efficiency or breaking the association between Glu152 and Mg^{2+} may lead to the development of TDP2 inhibitors with increased efficacy [24]. TDP2 can repair DSBs induced by radiomimetic drugs (Fig. 3). Therefore, TDP2 inhibition combined with a TOP1 inhibitor and radiomimetic drugs results in cancer cell sensitization. Based on the higher sensitivity of *TDP1*^{-/-}

TDP2^{E152Q/E152Q} cells to radiomimetic drugs than single mutants, breaking the bond between TDP2 and divalent metal ions may be important in radiomimetic drug therapy. Development of improved TDP2 inhibitors is anticipated in the future.

The TK6 mutant panel profile enabled us to identify important genes to be targeted for drug development. For example, *RAD54*^{-/-}/*LIG4*^{-/-} cells are the most sensitive mutant cells to X-rays and radiomimetic drugs, which confirms the synergistic combination of radiomimetic drugs and DSB repair inhibitors. Since numerous genes associated with DNA damage and repair responses are frequently altered in human cancers, identifying the faulty genes within each tumor cell is essential to enhance the efficacy of anticancer drugs. By selecting drugs that trigger DNA damage repair specific to the defective gene, we can expect a more potent cell-killing effect. The sensitivity profile of the TK6 mutants established in this study offers a logical method to assess the significance of individual repair pathways and genes as potential targets in chemotherapy.

The combination of TDP inhibitors with radiomimetic drugs such as Bleo shows promise as a therapeutic strategy but also presents several challenges. A primary concern is off-target toxicity: while TDP inhibitors enhance the efficacy of radiomimetic drugs by impairing specific DNA repair pathways, they may inadvertently disrupt other cellular processes, resulting in unintended harm to non-target cells. Moreover, resistance mechanisms can emerge during prolonged treatment. Cancer cells may acquire mutations or upregulate alternative repair pathways, such as NHEJ or HR, thereby diminishing the therapy's effectiveness. To address these limitations, the development of biomarkers for predicting and monitoring treatment responses is crucial. In addition, combination regimens must be carefully optimized to minimize off-target effects and delay resistance, for example by employing intermittent dosing schedules or incorporating agents that target alternative repair pathways.

Conclusions

In this study, we identified *TDP2* as a susceptible gene in the absence of *TDP1* to target cancers with radiomimetic drugs. TDP2 is important for the repair of radiomimetic drug-induced DSBs in the absence of TDP1. Elucidation of the TDP2-dependent repair pathway for DSBs induced by radiomimetic drugs revealed that the combination of radiomimetic drugs, TDP1 inhibitors, and TDP2 inhibitors can be used for cancer treatment. Further studies are needed to elucidate the detailed repair mechanism of TDP2 for DNA damage induced by radiomimetic drugs.

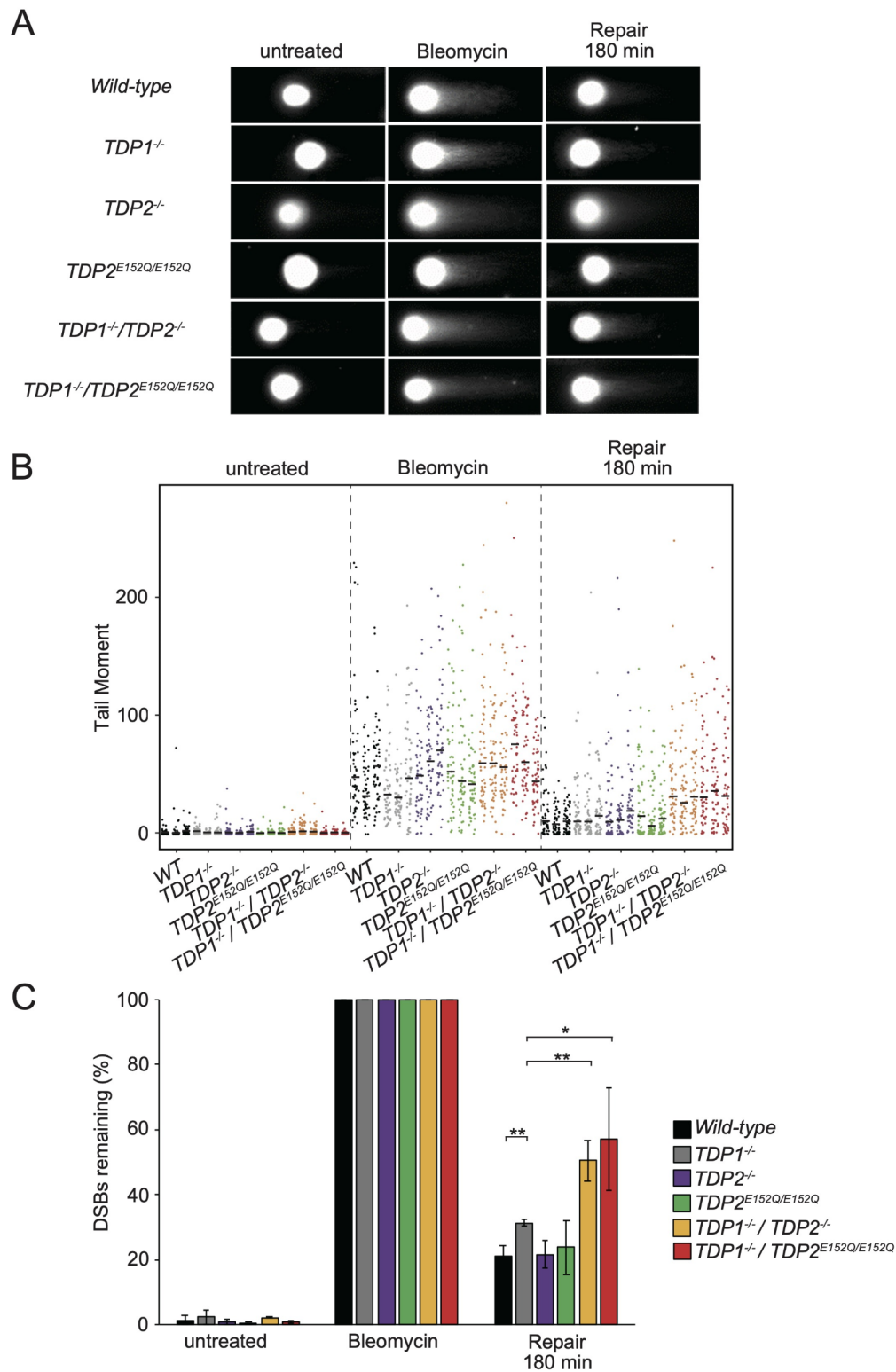


Fig. 3 Repair kinetics of DSBs in Bleo-treated cells. **A** Typical neutral comet images. The indicated cells treated with Bleo and not treated with Bleo (control) were analyzed for DSBs using neutral comet assays as described in the legend of Fig. 2A. **B** Tail moments were quantified as described in the legend of Fig. 2B. **C** DSBs remaining was calculated as described in the legend of Fig. 2C. Significant differences were identified using ANOVA and Student's t-test: ** $p < 0.01$, * $p < 0.05$. Median tail moments before standardization are shown in Fig. S1B

Abbreviations

BER	Base excision repair
Bleo	Bleomycin
CAL	Calicheamicin
CPT	Camptothecin
DPCs	DNA-protein crosslinks
DSBs	DNA double-strand breaks
HR	Homologous recombination
IR	Ionizing radiation
MMR	Mismatch repair
NER	Nucleotide excision repair
NHEJ	Nonhomologous end joining
3'-PG	3'-phosphoglycolate
SSBs	DNA single-strand breaks
TDP	Tyrosyl-DNA phosphodiesterase
TLS	Translesion DNA synthesis
TOP	Topoisomerase
TOP1ccs	TOP1-DNA cleavage complexes
TOP2ccs	TOP2-DNA cleavage complexes

Supplementary Information

The online version contains supplementary material available at <https://doi.org/10.1186/s41021-025-00329-9>.

Supplementary Material 1.
Supplementary Material 2.
Supplementary Material 3.
Supplementary Material 4.

Acknowledgements

The authors thank C. Kumagai (Hiroshima University) for their technical assistance. The authors are grateful to Dr. S. Takeda and Dr. H. Sasanuma (Kyoto University) for providing the TK6 cell lines.

Authors' contributions

MT conceptualized and initiated the project. MT, NS, MW, and KH conducted the experiments. MT drafted the manuscript. MT and KI curated the data. RM designed and edited the figures. MT, NS, KH, and KI contributed to the acquisition of funding. All authors reviewed and approved the final manuscript.

Funding

This work was supported by JSPS KAKENHI [grant numbers 20K19974, 22KK12374, and 19KK0210] (to M.T.), JSPS KAKENHI [grant number 22K18030] (to N.S.), JSPS KAKENHI [grant number 24K20936] (to K.I.), Health and Labor Sciences Research Grant [grant number 22KD2001] (to M.T.), KOSÉ Cosmetology Research Foundation (2020-22 to M.T.), Asahi Quality and Innovations (to M.T.), and Tokyo Metropolitan Government Advanced Research [grant Number R3-2] (to K.H.).

Data availability

The data generated and analyzed during the current study are available from the corresponding author on reasonable request.

Declarations

Ethics approval and consent to participate

Not applicable.

Consent for publication

Not applicable.

Competing interests

The authors declare no competing interests.

Received: 4 December 2024 / Accepted: 12 March 2025

Published online: 28 March 2025

References

1. Umezawa H, Maeda K, Takeuchi T, Okami Y. New antibiotics, bleomycin A and B. *J Antibiot (Tokyo)*. 1966;19(5):200–9.
2. Karpiński TM, Adamczak A. Anticancer activity of bacterial proteins and peptides. *Pharmaceutics* 2018;10(2):54.
3. Povirk LF. DNA damage and mutagenesis by radiomimetic DNA-cleaving agents: bleomycin, neocarzinostatin and other enediynes. *Mutat Res*. 1996;355(1–2):71–89.
4. Bradley MQ, Kohn KW. X-ray induced DNA double strand break production and repair in mammalian cells as measured by neutral filter elution. *Nucleic Acids Res*. 1979;7(3):793–804.
5. Chen J, Stubbe J. Bleomycins: towards better therapeutics. *Nat Rev Cancer*. 2005;5(2):102–12.
6. Jääskelä-Saari HA, Kairemo KJ, Jekunen AP, Pekkola-Heino K, Kulmala J, Ramsay HA, et al. Cytotoxicity of bleomycin and external radiation in squamous cell cancer cell lines of head and neck. *Cancer Detect Prev*. 1996;20(4):279–84.
7. Huang RX, Zhou PK. DNA damage response signaling pathways and targets for radiotherapy sensitization in cancer. *Signal Transduct Target Ther*. 2020;5(1):60.
8. Ceccaldi R, Rondinelli B, D'Andrea AD. Repair pathway choices and consequences at the Double-Strand break. *Trends Cell Biol*. 2016;26(1):52–64.
9. Morozumi R, Shimizu N, Tamura K, Nakamura M, Suzuki A, Ishiniwa H, et al. Changes in repair pathways of radiation-induced DNA double-strand breaks at the midblastula transition in xenopus embryo. *J Radiat Res*. 2024;65(3):315–22.
10. Wright WD, Shah SS, Heyer WD. Homologous recombination and the repair of DNA double-strand breaks. *J Biol Chem*. 2018;293(27):10524–35.
11. Crickard JB. Discrete roles for Rad54 and Rdh54 during homologous recombination. *Curr Opin Genet Dev*. 2021;71:48–54.
12. Pannunzio NR, Watanabe G, Lieber MR. Nonhomologous DNA end-joining for repair of DNA double-strand breaks. *J Biol Chem*. 2018;293(27):10512–23.
13. Mirza-Aghazadeh-Attari M, Mohammadzadeh A, Yousefi B, Mihanfar A, Karimian A, Majidinia M. 53BP1: A key player of DNA damage response with critical functions in cancer. *DNA Repair (Amst)*. 2019;73:110–9.
14. Krokan HE, Bjørås M. Base excision repair. *Cold Spring Harb Perspect Biol*. 2013;5(4):a012583.
15. Morales J, Li L, Fattah FJ, Dong Y, Bey EA, Patel M, et al. Review of Poly (ADP-ribose) Polymerase (PARP) mechanisms of action and rationale for targeting in cancer and other diseases. *Crit Rev Eukaryot Gene Expr*. 2014;24(1):15–28.
16. Demin AA, Hirota K, Tsuda M, Adamowicz M, Hailstone R, Brazina J, et al. XRCC1 prevents toxic PARP1 trapping during DNA base excision repair. *Mol Cell*. 2021;81(14):3018–e305.
17. El-Khamisy SF, Masutani M, Suzuki H, Caldecott KW. A requirement for PARP-1 for the assembly or stability of XRCC1 nuclear foci at sites of oxidative DNA damage. *Nucleic Acids Res*. 2003;31(19):5526–33.
18. Tsuda M, Cho K, Ooka M, Shimizu N, Watanabe R, Yasui A, et al. ALC1/CHD1L, a chromatin-remodeling enzyme, is required for efficient base excision repair. *PLoS ONE*. 2017;12(11):e0188320.
19. Sobol RW, Horton JK, Kühn R, Gu H, Singhal RK, Prasad R, et al. Requirement of mammalian DNA polymerase-beta in base-excision repair. *Nature*. 1996;379(6561):183–6.
20. Caldecott KW, Aoufouchi S, Johnson P, Shall S. XRCC1 Polypeptide interacts with DNA Polymerase beta and possibly Poly (ADP-ribose) Polymerase, and DNA ligase III is a novel molecular 'nick-sensor' in vitro. *Nucleic Acids Res*. 1996;24(22):4387–94.
21. Vaz B, Popovic M, Newman JA, Fielden J, Aitkenhead H, Halder S, et al. Metalloprotease SPRTN/DVC1 orchestrates Replication-Coupled DNA-Protein crosslink repair. *Mol Cell*. 2016;64(4):704–19.
22. Tsuda M, Shimizu N, Tomikawa H, Morozumi R, Ide H. Repair pathways for radiation DNA damage under normoxic and hypoxic conditions: assessment with a panel of repair-deficient human TK6 cells. *J Radiat Res* 2021;62(6):999–1004.
23. Honma M, Hayashi M. Comparison of in vitro micronucleus and gene mutation assay results for p53-competent versus p53-deficient human lymphoblastoid cells. *Environ Mol Mutagen*. 2011;52(5):373–84.
24. Shimizu N, Hamada Y, Morozumi R, Yamamoto J, Iwai S, Sugiyama KI, et al. Repair of topoisomerase 1-induced DNA damage by tyrosyl-DNA phosphodiesterase 2 (TDP2) is dependent on its magnesium binding. *J Biol Chem*. 2023;299(8):104988.
25. Honma M. Generation of loss of heterozygosity and its dependency on p53 status in human lymphoblastoid cells. *Environ Mol Mutagen*. 2005;45(2–3):162–76.

26. Tsuda M, Ogawa S, Ooka M, Kobayashi K, Hirota K, Wakasugi M, et al. PDIP38/PolDIP2 controls the DNA damage tolerance pathways by increasing the relative usage of translesion DNA synthesis over template switching. *PLoS ONE*. 2019;14(3):e0213383.
27. Ji K, Kogame T, Choi K, Wang X, Lee J, Taniguchi Y, et al. A novel approach using DNA-repair-deficient chicken DT40 cell lines for screening and characterizing the genotoxicity of environmental contaminants. *Environ Health Perspect*. 2009;117(11):1737–44.
28. Tsuda M, Terada K, Ooka M, Kobayashi K, Sasanuma H, Fujisawa R, et al. The dominant role of proofreading exonuclease activity of replicative polymerase ϵ in cellular tolerance to cytarabine (Ara-C). *Oncotarget*. 2017;8(20):33457–74.
29. Gyori BM, Venkatachalam G, Thiagarajan PS, Hsu D, Clement MV. OpenComet: an automated tool for comet assay image analysis. *Redox Biol*. 2014;2:457–65.
30. Tsuda M, Kitamasu K, Kumagai C, Sugiyama K, Nakano T, Ide H. Tyrosyl-DNA phosphodiesterase 2 (TDP2) repairs topoisomerase 1 DNA-protein crosslinks and 3'-blocking lesions in the absence of tyrosyl-DNA phosphodiesterase 1 (TDP1). *DNA Repair (Amst)*. 2020;91–2:102849.
31. Hsiang YH, Hertzberg R, Hecht S, Liu LF. Camptothecin induces protein-linked DNA breaks via mammalian DNA topoisomerase I. *J Biol Chem*. 1985;260(27):14873–8.
32. Pommier Y, Leo E, Zhang H, Marchand C. DNA topoisomerases and their poisoning by anticancer and antibacterial drugs. *Chem Biol*. 2010;17(5):421–33.
33. Meisenberg C, Gilbert DC, Chalmers A, Haley V, Gollins S, Ward SE, et al. Clinical and cellular roles for TDP1 and TOP1 in modulating colorectal cancer response to Irinotecan. *Mol Cancer Ther*. 2015;14(2):575–85.
34. Tsuda M, Kitamasu K, Hosokawa S, Nakano T, Ide H. Repair of trapped topoisomerase II covalent cleavage complexes: novel proteasome-independent mechanisms. *Nucleosides Nucleotides Nucleic Acids*. 2020;39(1–3):170–84.
35. Zeng Z, Sharma A, Ju L, Murai J, Umans L, Vermeire L, et al. TDP2 promotes repair of topoisomerase I-mediated DNA damage in the absence of TDP1. *Nucleic Acids Res*. 2012;40(17):8371–80.
36. Hoa NN, Shimizu T, Zhou ZW, Wang ZQ, Deshpande RA, Paull TT, et al. Mre11 is essential for the removal of lethal topoisomerase 2 covalent cleavage complexes. *Mol Cell*. 2016;64(3):580–92.
37. Akagawa R, Trinh HT, Saha LK, Tsuda M, Hirota K, Yamada S, et al. UBC13-Mediated Ubiquitin Signaling Promotes Removal of Blocking Adducts from DNA Double-Strand Breaks. *iScience*. 2020;23(4):101027.
38. Sasanuma H, Tsuda M, Morimoto S, Saha LK, Rahman MM, Kiyooka Y, et al. BRCA1 ensures genome integrity by eliminating estrogen-induced pathological topoisomerase II-DNA complexes. *Proc Natl Acad Sci U S A*. 2018;115(45):E10642–51.
39. Keka IS, Mohiuddin, Maede Y, Rahman MM, Sakuma T, Honma M, et al. Smarcal1 promotes double-strand-break repair by nonhomologous end-joining. *Nucleic Acids Res*. 2015;43(13):6359–72.
40. Saha LK, Kim S, Kang H, Akter S, Choi K, Sakuma T, et al. Differential micronucleus frequency in isogenic human cells deficient in DNA repair pathways is a valuable indicator for evaluating genotoxic agents and their genotoxic mechanisms. *Environ Mol Mutagen*. 2018;59(6):529–38.
41. Hu Q, Klages-Mundt N, Wang R, Lynn E, Kuma Saha L, Zhang H, et al. The ARK assay is a sensitive and versatile method for the global detection of DNA-Protein crosslinks. *Cell Rep*. 2020;30(4):1235–e454.
42. Rahman MM, Mohiuddin M, Shamima Keka I, Yamada K, Tsuda M, Sasanuma H, et al. Genetic evidence for the involvement of mismatch repair proteins, PMS2 and MLH3, in a late step of homologous recombination. *J Biol Chem*. 2020;295(51):17460–75.
43. Olive PL, Ban ath JP. The comet assay: a method to measure DNA damage in individual cells. *Nat Protoc*. 2006;1(1):23–9.
44. Hawkins AJ, Subler MA, Akopiants K, Wiley JL, Taylor SM, Rice AC, et al. In vitro complementation of Tdp1 deficiency indicates a stabilized enzyme-DNA adduct from Tyrosyl but not glycolate lesions as a consequence of the SCAN1 mutation. *DNA Repair (Amst)*. 2009;8(5):654–63.
45. Interthal H, Chen HJ, Champoux JJ. Human Tdp1 cleaves a broad spectrum of substrates, including phosphoamide linkages. *J Biol Chem*. 2005;280(43):36518–28.
46. Huang SY, Murai J, Dalla Rosa I, Dexheimer TS, Naumova A, Gmeiner WH, et al. TDP1 repairs nuclear and mitochondrial DNA damage induced by chain-terminating anticancer and antiviral nucleoside analogs. *Nucleic Acids Res*. 2013;41(16):7793–803.
47. Murai J, Huang SY, Das BB, Dexheimer TS, Takeda S, Pommier Y. Tyrosyl-DNA phosphodiesterase 1 (TDP1) repairs DNA damage induced by topoisomerases I and II and base alkylation in vertebrate cells. *J Biol Chem*. 2012;287(16):12848–57.
48. Inamdar KV, Pouliot JJ, Zhou T, Lees-Miller SP, Rasouli-Nia A, Povirk LF. Conversion of phosphoglycolate to phosphate termini on 3' overhangs of DNA double strand breaks by the human tyrosyl-DNA phosphodiesterase hTdp1. *J Biol Chem*. 2002;277(30):27162–8.
49. Zhou T, Akopiants K, Mohapatra S, Lin PS, Valerie K, Ramsden DA, et al. Tyrosyl-DNA phosphodiesterase and the repair of 3'-phosphoglycolate-terminated DNA double-strand breaks. *DNA Repair (Amst)*. 2009;8(8):901–11.
50. Kawale AS, Akopiants K, Valerie K, Ruis B, Hendrickson EA, Huang SN, et al. TDP1 suppresses mis-joining of radiomimetic DNA double-strand breaks and cooperates with Artemis to promote optimal nonhomologous end joining. *Nucleic Acids Res*. 2018;46(17):8926–39.

Publisher's Note

Springer Nature remains neutral with regard to jurisdictional claims in published maps and institutional affiliations.